International Journal of Injury Control and Safety Promotion

ISSN: (Print) (Online) Journal homepage: https://www.tandfonline.com/loi/nics20

Monitoring road accident and injury using indeterminacy based Shewhart control chart using multiple dependent state repetitive sampling

Nasrullah Khan & Muhammad Aslam

INTERNATIONAL JOURNAL OF INJURY CONTROL AND SAFETY PROMOTION
https://doi.org/10.1080/17457300.2022.2029911

Taylor & Francis
Taylor & Francis Group

RESEARCH ARTICLE

Check for updates

Monitoring road accident and injury using indeterminacy based Shewhart control chart using multiple dependent state repetitive sampling

Nasrullah Khan[a] and Muhammad Aslam[b]

[a]Department of Statistics, University of Veterinary and Animal Sciences, Lahore, Pakistan; [b]Department of Statistics, Faculty of Science, King Abdulaziz University, Jeddah, Saudi Arabia

ABSTRACT

The uncertainty/indeterminate in control chart parameter/observations affects the performance of the control chart. This paper addresses the indeterminacy and its effect on the Shewhart X-bar control using multiple dependent state repetitive sampling. The probabilities and neutrosophic average run length for in-control and out-of-control processes are derived. The tables and figures of the proposed chart are presented when uncertainty/indeterminate is present in sample size and proceeding subgroups. The efficiency of the proposed chart is compared with the existing charts and the proposed chart is found to be efficient in terms of neutrosophic average run length.

ARTICLE HISTORY
Received 24 September 2021
Revised 28 December 2021
Accepted 12 January 2022

KEYWORDS
Shewhart chart; neutrosophic; simulation; classical statistics; neutrosophic average run length

1. Introduction

In the modern era, the industries are competing with each other in terms of the quality of the product. The reputation of the industry depends on the quality of the products they produced. For the high-quality products, some specifications are set by the industrialists. Therefore, the monitoring of the set specifications is done by using the control charts. The control charts are helpful to keep the process at the target specification. The Shewhart control charts are common to apply in the industry for monitoring the industrial process. These types of control charts are helpful to monitor the change in average and variation in the industrial process. The control charts give an indication of when the process is shifted due to some cause of variations. The timely indication about the shift in the process minimizes the non-conforming product. In nutshell, the control charts are an important tool to maintain the high quality of the product. Bai and Lee (2002), He et al. (2002), Wu and Wang (2007), Zarandi et al. (2008), Ertuğrul and Aytaç (2009), Kaya (2009), Ahmad et al. (2014), Joekes and Barbosa (2013), Ho and Quinino (2013), and Aldosari et al. (2017) worked on Shewhart control charts. It is important to note that the Shewhart control charts are less effective to detect a small shift in the process.

As pointed by Aslam et al. (2019a) that the efficiency of the Shewhart control chart can be increased by incorporating various sampling schemes. In the Shewhart control chart, usually, the charts are designed using the single sampling where the decision about the state of the chart is taken on the basis of a single sample. Sherman (1965) introduced the multiple dependent state (MDS) sampling plan that was found to be efficient in the area of the control chart, see Aslam, Nazir, et al. (2015), Aslam, Azam, et al. (2015), Aslam et al. (2017), and Aldosari et al. (2017). The repetitive sampling scheme is applied when no decision about the state of the process is made on the first sample and found to be effective for Shewhart control charts, see Ahmad et al. (2014) and Adeoti (2018). Aldosari et al. (2017) and Aldosari et al. (2018) introduced the charts by integrated MDS and repetitive sampling schemes.

Senturk and Erginel (2009) mentioned that 'observations include human judgments, and evaluations and decisions, a continuous random variable of a production process should include the variability caused by human subjectivity or measurement devices, or environmental conditions. These variability causes create vagueness in the measurement system'. Therefore, in the presence of uncertainty in sample size or proceeding subgroups, the aforementioned control chart using classical statistics cannot be applied for monitoring the process. To handle the situation of uncertainty, the fuzzy-approach based control chart can be applied for monitoring of the industrial process. Zarandi et al. (2008), Ertuğrul and Aytaç (2009), Gülbay et al. (2004), Ertuğru and Güneş (2007), Engin et al. (2008), Faraz et al. (2010), Avakh Darestani et al. (2014), Mojtaba Zabihinpour et al. (2015), Fernández (2017, pp. 1–6), Alakoc and Apaydin (2018), Ercan Teksen and Anagun (2018), and Fadaei and Pooya (2018) contributed excellent works in the area of fuzzy-based control charts.

The neutrosophic logic is more efficient than fuzzy logic in terms of information. The neutrosophic logic gives information about the measure of truth, the measure of indeterminacy, and the measure of falseness. Smarandache (2010), Abdel-Basset, Atef et al. (2019), Abdel-Basset, Gunasekaran, et al. (2019), Abdel-Basset et al. (2018), and

CONTACT Muhammad Aslam aslam_ravian@hotmail.com

Abdel-Basset et al. (2020) studied various applications using neutrosophic logic. Smarandache (2014) introduced the idea of neutrosophic statistics and showed that it is efficient than classical statistics. The neutrosophic statistics applied when the data are uncertain, imprecise, and indeterminate. Aslam et al. (2018), Aslam (2019a, 2019b), Aslam et al. (2019b), and Aslam and Khan (2019) proposed the control charts using neutrosophic statistics. Aslam et al. (2019a) proposed the control chart using MDS under neutrosophic statistics. Aslam (2019c) proposed the control chart using repetitive sampling under neutrosophic statistics

A rich literature on control charts using multiple dependent state repetitive sampling (MDSRS) under classical statistics is available. By exploring the literature and according to the best of the authors' knowledge, the Shewhart X-bar control chart using MDSRS under neutrosophic statistics was not explored yet. In this paper, the Shewhart X-bar control chart using MDSRS under neutrosophic statistics will be designed. The probabilities of in-control and out-of-control of the proposed chart will be derived. The efficiency of the proposed chart is discussed in terms of neutrosophic average run length (NARL). The application of the proposed chart is given using the road accidents and road injuries data. It is expected that the proposed Shewhart X-bar control chart using MDSRS under neutrosophic statistics will be efficient than the existing control charts in terms if NARL.

2. Methodology of the proposed chart

Suppose that $X_N = X_L + X_U I_{XN}; I_{XN}\epsilon\left[I_{XL}, I_{XU}\right]$ be the neutrosophic random variable of neutrosophic sample size $n_N = n_L + n_U I_{nN}; I_{nN}\epsilon\left[I_{nL}, I_{nU}\right]$ follows the neutrosophic normal distribution with neutrosophic mean $\mu_N = \mu_L + \mu_U I_{\mu N}; I_{\mu N}\epsilon\left[I_{\mu L}, I_{\mu U}\right]$ and neutrosophic standard deviation $\sigma_N = \sigma_L + \sigma_U I_{\sigma N}; I_{\sigma N}\epsilon\left[I_{\sigma L}, I_{\sigma U}\right]$. Suppose that $\overline{X}_N = \overline{X}_L + \overline{X}_U I_{\overline{X}N}; I_{\overline{X}N}\epsilon\left[I_{\overline{X}L}, I_{\overline{X}U}\right]$ and $s_N = s_L + s_U I_{sN}; I_{sN}\epsilon\left[I_{sL}, I_{sU}\right]$ be the neutrosophic sample mean and neutrosophic sample standard deviation. Suppose that $m_N = m_L + m_U I_{mN}; I_{mN}\epsilon\left[I_{mL}, I_{mU}\right]$ be neutrosophic target value. Note that in all the above neutrosophic forms, the first value denotes the determined values and the second value is indeterminate values. Based on the information, the neutrosophic control limits are defined as

$$LCL_{1N} = m_N - k_{1N}\frac{\sigma_N}{\sqrt{n_N}};\ \mu_N\epsilon\left[\mu_L, \mu_U\right], \sigma_N\epsilon\left[\sigma_L, \sigma_U\right], m_N\epsilon\left[m_L, m_U\right] \quad (1)$$

$$UCL_{1N} = m_N + k_{1N}\frac{\sigma_N}{\sqrt{n_N}};\mu_N\epsilon\left[\mu_L, \mu_U\right], \sigma_N\epsilon\left[\sigma_L, \sigma_U\right], m_N\epsilon\left[m_L, m_U\right] \quad (2)$$

$$LCL_{2N} = m_N - k_{2N}\frac{\sigma_N}{\sqrt{n_N}};\ \mu_N\epsilon\left[\mu_L, \mu_U\right], \sigma_N\epsilon\left[\sigma_L, \sigma_U\right], m_N\epsilon\left[m_L, m_U\right] \quad (3)$$

$$UCL_{2N} = m_N + k_{2N}\frac{\sigma_N}{\sqrt{n_N}};\ \mu_N\epsilon\left[\mu_L, \mu_U\right], \sigma_N\epsilon\left[\sigma_L, \sigma_U\right], m_N\epsilon\left[m_L, m_U\right] \quad (4)$$

where $k_{1N}\epsilon\left[k_{1L}, k_{1U}\right]$ and $k_{2N}\epsilon\left[k_{2L}, k_{2U}\right]$ are neutrosophic control limits coefficients.

The MDSRS under neutrosophic statistics is mentioned as follows

Step-1: Select a random sample of size $n_N = n_L + n_U I_{nN}; I_{nN}\epsilon\left[I_{nL}, I_{nU}\right]$ and compute $\overline{X}_N = \overline{X}_L + \overline{X}_U I_{\overline{X}N}; I_{\overline{X}N}\epsilon\left[I_{\overline{X}L}, I_{\overline{X}U}\right]$

Step-2: Declare the process in-control $LCL_{2N} \le \overline{X}_N \le UCL_{2N}$ and out-of-control if $\overline{X}_N \ge UCL_{1N}$ or $\overline{X}_N \le UCL_{1N}$.

Step-3: If $UCL_{2N} \le \overline{X} \le UCL_{1N}$ or $LCL_{1N} \le \overline{X} \le LCL_{2N}$, declare the process is incontrol if $i_N = i_L + i_U I_{iN}; I_{iN}\epsilon\left[I_{iL}, I_{iU}\right]$ subgroups are incontrol, otherwise, declare the process out-of-control.

Note that the industrial engineers are uncertain about previous subgroups $i_N = i_L + i_U I_{iN}; I_{iN}\epsilon\left[I_{iL}, I_{iU}\right]$ and sample size $n_N = n_L + n_U I_{nN}; I_{nN}\epsilon\left[I_{nL}, I_{nU}\right]$. The operational decision about the state of the process is based on four control limits. The proposed chart is the generalization of the chart using MDS sampling and repetitive sampling scheme under neutrosophic statistics. Let $\mu_N\epsilon\left[\mu_L, \mu_U\right] = m_N\epsilon\left[m_L, m_U\right]$ be the target neutrosophic average. For single sampling, the probability that the process is an in-control state by following (Aldosari et al., 2018) is given

$$P^0_{in,1N} = P\left(LCL_{2N} \le \overline{X}_N \le UCL_{2N}\right) + \begin{Bmatrix} P\left(LCL_{1N} < \overline{X}_N < LCL_{2N}\right) + \\ P\left(UCL_{2N} < \overline{X}_N < UCL_{1N}\right) \end{Bmatrix} \left\{P\left(LCL_{2N} \le \overline{X}_N \le UCL_{2N}\right)\right\}^{i_N};\ i_N\epsilon\left[i_L, i_U\right] \quad (5)$$

The simplified form of $P^0_{in,1N}$ by following (Aldosari et al., 2018) is given by

$$P^0_{in,1N} = \left(2\Phi_N\left(k2_N\right) - 1\right) + 2\left\{\Phi_N\left(k1_N\right) - \Phi_N\left(k2_N\right)\right\} \left\{2\Phi_N\left(k2_N\right) - 1\right\}^{i_N};\ i_N\epsilon\left[i_L, i_U\right] \quad (6)$$

The probability of in-control under resampling is given by

$$P^0_{repN} = \begin{Bmatrix} P\left(LCL_{1N} < \overline{X}_N < LCL_{2N}\right) \\ + P\left(UCL_{2N} < \overline{X}_N < UCL_{1N}\right) \end{Bmatrix} \left(1 - \left[P\left\{LCL_{2N} \le \overline{X}_N \le UCL_{2N}\right\}\right]^{i_N}\right);\ i_N\epsilon\left[i_L, i_U\right] \quad (7)$$

The simplified form of P^0_{repN} by following (Aldosari et al., 2018) is given by

$$P^0_{repN} = 2\left\{\Phi_N\left(k_{1N}\right) - \Phi_N\left(1k_N\right)\right\}\left(1 - \left[2\Phi_N\left(k_{2N}\right) - 1\right]^{i_N}\right); i_N\epsilon\left[i_L, i_U\right] \quad (8)$$

where $\Phi_N\left(x_N\right)$ presents the cumulative distribution function of the neutrosophic standard deviation. The probability of in-control for MDSRS under neutrosophic statistics is given by

$$P_{inN}^{0}=\frac{P_{in,1N}^{0}}{1-P_{repN}^{0}}=\frac{\begin{pmatrix}2\Phi_N\\(k_{2N})-1\end{pmatrix}+2\begin{Bmatrix}\Phi_N(k_{1N})\\-\Phi_N(k_{1N})\end{Bmatrix}\begin{Bmatrix}2\Phi_N\\(k_{2N})-1\end{Bmatrix}^{i_N}}{1-2\begin{Bmatrix}\Phi_N(k_{1N})\\-\Phi_N(k_{2N})\end{Bmatrix}\left(1-\begin{bmatrix}2\Phi_N\\(k_{2N})-1\end{bmatrix}^{i_N}\right)};\quad i_N\epsilon[i_L,i_U] \tag{9}$$

The neutrosophic average run length for the in-control process is defined as

$$ARL_{0N}=\frac{1}{1-\dfrac{\begin{pmatrix}2\Phi_N\\(k_{2N})-1\end{pmatrix}+2\begin{Bmatrix}\Phi_N(k_{1N})\\-\Phi_N(k_{2N})\end{Bmatrix}\begin{Bmatrix}2\Phi_N\\(k_{2N})-1\end{Bmatrix}^{i_N}}{1-2\begin{Bmatrix}\Phi_N(k_{1N})\\-\Phi_N(k_{2N})\end{Bmatrix}\left(1-\begin{bmatrix}2\Phi_N\\(k_{2N})-1\end{bmatrix}^{i_N}\right)}};\quad i_N\epsilon[i_L,i_U] \tag{10}$$

Suppose that the process has shifted to new neutrosophic mean $\mu_{1N}=m_N+c\sigma_N$, where c is a shift constant. For single sampling, the probability that the process is the in-control state for the shifted process by following (Aldosari et al., 2018) is given

$$P_{in,1N}^{1}\mid\mu_{1N}=P\begin{pmatrix}\Phi_N\left(k_{2N}-c\sqrt{n_N}\right)\\+\Phi\left(k_{2N}+c\sqrt{n_N}\right)-1\end{pmatrix}+\begin{bmatrix}\Phi_N\left(k_{1N}+c\sqrt{n_N}\right)\\-\Phi_N\left(k_{2N}+c\sqrt{n_N}\right)\\+\Phi_N\left(k_{1N}-c\sqrt{n_N}\right)\\-\Phi_N\left(k_{2N}-c\sqrt{n_N}\right)\end{bmatrix} \tag{11}$$

$$s\left\{\begin{pmatrix}\Phi_N\left(k_{2N}-c\sqrt{n}\right)+\\\Phi_N\left(k_{2N}+c\sqrt{n}\right)-1\end{pmatrix}\right\}^{i_N};\quad i_N\epsilon[i_L,i_U],n_N\epsilon[n_L,n_U]$$

The probability of in-control at μ_{1N} under resampling is given by

$$P_{repN}^{1}=\begin{bmatrix}\Phi_N\left(k_{1N}+c\sqrt{n_N}\right)\\-\Phi_N\left(k_{1N}+c\sqrt{n_N}\right)\\+\Phi_N\left(k_{1N}-c\sqrt{n_N}\right)\\-\Phi_N\left(k_{2N}-c\sqrt{n_N}\right)\end{bmatrix}\left(1-\begin{bmatrix}\Phi_N\left(k_{2N}-c\sqrt{n_N}\right)\\+\Phi_N\left(k_{2N}+c\sqrt{n_N}\right)-1\end{bmatrix}^{i_N}\right),\quad i_N\epsilon[i_L,i_U],n_N\epsilon[n_L,n_U] \tag{12}$$

The probability of in-control for MDSRS at μ_{1N} under neutrosophic statistics is given by

$$P_{inN}^{1}=\frac{P_{in,1N}^{1}}{1-P_{repN}^{1}}=\frac{\begin{pmatrix}\Phi_N\left(k_{2N}-c\sqrt{n}\right)\\+\Phi_N\left(k_{2N}+c\sqrt{n}\right)-1\end{pmatrix}+2\begin{Bmatrix}\left(k_{1N}+c\sqrt{n}\right)\\-\left(k_{2N}+c\sqrt{n}\right)\end{Bmatrix}\left\{\begin{pmatrix}\Phi_N\left(k_{2N}-c\sqrt{n}\right)+\\\Phi_N\left(k_{2N}+c\sqrt{n}\right)-1\end{pmatrix}\right\}^{i_N}}{1-\begin{bmatrix}\Phi_N\left(k_{1N}+c\sqrt{n_N}\right)-\Phi_N\left(k_{2N}+c\sqrt{n_N}\right)\\+\Phi_N\left(k_{1N}-c\sqrt{n_N}\right)-\Phi_N\left(k_{2N}-c\sqrt{n_N}\right)\end{bmatrix}(1-i_N)};\quad i_N\epsilon[i_L,i_U],n_N\epsilon[n_L,n_U] \tag{13}$$

The neutrosophic average run length for the in-control process is defined as

$$ARL_{1N}=\frac{1}{1-\left\{\dfrac{\begin{pmatrix}\Phi_N\left(k_{2N}-c\sqrt{n}\right)\\+\Phi_N\left(k_{2N}+c\sqrt{n}\right)-1\end{pmatrix}+2\begin{Bmatrix}\left(k_{1N}+c\sqrt{n}\right)\\-\left(k_{2N}+c\sqrt{n}\right)\end{Bmatrix}\left\{\begin{pmatrix}\Phi_N\left(k_{2N}-c\sqrt{n}\right)+\\\Phi_N\left(k_{2N}+c\sqrt{n}\right)-1\end{pmatrix}\right\}^{i_N}}{1-\begin{bmatrix}\Phi_N\left(k_{1N}+c\sqrt{n_N}\right)-\Phi_N\left(k_{2N}+c\sqrt{n_N}\right)\\+\Phi_N\left(k_{1N}-c\sqrt{n_N}\right)-\Phi_N\left(k_{2N}-c\sqrt{n_N}\right)\end{bmatrix}(1-i_N)}\right\}};\quad i_N\epsilon[i_L,i_U],n_N\epsilon[n_L,n_U] \tag{14}$$

Suppose that $ARL_{0N}=r_{0N}$ be the specified NARL. The values of $ARL_{1N}\epsilon[ARL_{1L},ARL_{1U}]$ for various values of c, $i_N\epsilon[i_L,i_U]$, $n_N\epsilon[n_L,n_U]$ and r_{0N} are placed in Tables 1–3. From Tables 1–3, the following trends can be observed.

1. For the other same values of $i_N\epsilon[i_L,i_U]$, r_{0N} and c, the values of $ARL_{1N}\epsilon[ARL_{1L},ARL_{1U}]$ decrease as $n_N\epsilon[n_L,n_U]$ increases.
2. For the other same values, the values of $ARL_{1N}\epsilon[ARL_{1L},ARL_{1U}]$ decrease as c increases.

The following algorithm under neutrosophic statistics was applied to generate the values of $ARL_{1N}\epsilon[ARL_{1L},ARL_{1U}]$.

Step-1: Set $ARL_{0N}=r_{0N}$, c, $i_N\epsilon[i_L,i_U]$ and $n_N\epsilon[n_L,n_U]$ and determine $k_{1N}\epsilon[k_{1L},k_{1U}]$ and $k_{2N}\epsilon[k_{2L},k_{2U}]$ such that

Table 1. The values of NARL when $n_N \epsilon [2,5]$ and $i_N \epsilon [2,4]$.

k_{1N}	[2.8463,2.8569]	[2.9663,2.9742]	[3.0237,3.0271]
k_{2N}	[1.1671,1.2112]	[1.1954,1.2762]	[1.2676,1.3961]
c		NARL	
0	[200.17,200.63]	[300.66,300.24]	[370.73,372.12]
0.02	[199.42,198.73]	[299.46,297.21]	[369.21,368.28]
0.03	[198.5,196.4]	[297.97,293.49]	[367.31,363.58]
0.05	[195.6,189.25]	[293.29,282.12]	[361.37,349.21]
0.06	[193.65,184.59]	[290.14,274.73]	[357.39,339.88]
0.08	[188.83,173.56]	[282.39,257.33]	[347.57,317.98]
0.1	[182.93,160.93]	[272.94,237.55]	[335.62,293.15]
0.12	[176.14,147.46]	[262.1,216.63]	[321.95,266.96]
0.15	[164.71,127.07]	[243.97,185.27]	[299.14,227.88]
0.2	[143.92,95.96]	[211.33,138.17]	[258.27,169.55]
0.25	[122.99,70.79]	[178.94,100.73]	[217.97,123.45]
0.3	[103.5,51.66]	[149.2,72.7]	[181.18,89.08]
0.4	[71.39,27.33]	[101.08,37.64]	[122.12,46.18]
0.5	[48.48,14.65]	[67.5,19.71]	[81.24,24.19]
0.6	[32.81,8.12]	[44.95,10.61]	[53.95,12.97]
0.7	[22.25,4.75]	[29.99,5.98]	[35.91,7.24]
0.8	[15.17,2.99]	[20.1,3.61]	[24.01,4.29]
0.9	[10.43,2.06]	[13.56,2.38]	[16.15,2.75]
0.95	[8.69,1.78]	[11.18,2.01]	[13.29,2.28]
1	[7.26,1.57]	[9.25,1.73]	[10.96,1.94]

Table 2. The values of NARL when $n_N \epsilon [5,7]$ and $i_N \epsilon [2,4]$.

k_{1N}	[2.8250,2.8368]	[2.9633,2.9768]	[3.0301,3.0318]
k_{2N}	[1.3696,1.3720]	[1.2219,1.2595]	[1.2094,1.3400]
c		NARL	
0	[200.54,200.37]	[300.24,300.71]	[372.31,371.37]
0.02	[198.74,197.79]	[297.27,296.46]	[368.47,365.98]
0.03	[196.52,194.65]	[293.63,291.29]	[363.77,359.44]
0.05	[189.72,185.16]	[282.47,275.75]	[349.4,339.8]
0.06	[185.27,179.09]	[275.21,265.86]	[340.07,327.34]
0.08	[174.75,165.08]	[258.13,243.22]	[318.17,298.88]
0.1	[162.66,149.63]	[238.68,218.53]	[293.34,267.97]
0.12	[149.73,133.8]	[218.08,193.56]	[267.17,236.84]
0.15	[130.07,111.05]	[187.16,158.23]	[228.11,193.03]
0.2	[99.83,78.94]	[140.56,109.58]	[169.83,133.12]
0.25	[75.07,55.13]	[103.33,74.51]	[123.77,90.24]
0.3	[55.97,38.3]	[75.28,50.39]	[89.41,60.88]
0.4	[31.03,18.64]	[39.75,23.21]	[46.42,27.9]
0.5	[17.39,9.39]	[21.14,11.05]	[24.26,13.17]
0.6	[9.94,5.04]	[11.43,5.61]	[12.87,6.57]
0.7	[5.86,2.97]	[6.38,3.14]	[7.04,3.59]
0.8	[3.63,1.97]	[3.77,2.01]	[4.06,2.22]
0.9	[2.42,1.48]	[2.42,1.48]	[2.54,1.58]
0.95	[2.04,1.34]	[2.01,1.33]	[2.1,1.4]
1	[1.77,1.24]	[1.73,1.22]	[1.78,1.27]

Table 3. The values of NARL when $n_N \epsilon [8,12]$ and $i_N \epsilon [2,4]$.

k_{1N}	[2.8123,2.8148]	[2.9587,2.9607]	[3.0243,3.0282]
k_{2N}	[1.7351,1.7382]	[1.3421,1.4226]	[1.3371,1.3698]
c		NARL	
0	[200.8,200.31]	[305.02,301.63]	[377.76,370.5]
0.02	[198,196.11]	[300.27,294.56]	[371.64,361.42]
0.03	[194.59,191.07]	[294.51,286.11]	[364.22,350.6]
0.05	[184.37,176.38]	[277.3,261.69]	[342.14,319.43]
0.06	[177.88,167.4]	[266.46,246.89]	[328.26,300.64]
0.08	[163.07,147.8]	[241.92,215.01]	[296.99,260.36]
0.1	[146.97,127.84]	[215.6,183.09]	[263.64,220.37]
0.12	[130.75,109.03]	[189.45,153.54]	[230.7,183.62]
0.15	[107.88,84.52]	[153.2,115.85]	[185.38,137.2]
0.2	[76.45,54.37]	[104.68,70.98]	[125.37,82.68]
0.25	[53.69,34.95]	[70.63,43.27]	[83.75,49.56]
0.3	[37.81,22.66]	[47.6,26.53]	[55.89,29.86]
0.4	[19.2,9.94]	[21.87,10.4]	[25.17,11.3]
0.5	[10.13,4.76]	[10.33,4.54]	[11.63,4.76]
0.6	[5.6,2.62]	[5.15,2.37]	[5.65,2.41]
0.7	[3.31,1.71]	[2.83,1.54]	[3.02,1.53]
0.8	[2.15,1.31]	[1.81,1.21]	[1.88,1.2]
0.9	[1.57,1.14]	[1.36,1.08]	[1.38,1.08]
0.95	[1.4,1.09]	[1.24,1.05]	[1.25,1.05]
1	[1.28,1.06]	[1.16,1.03]	[1.17,1.03]

Table 4. NARLs of three charts when $n_N \epsilon [5,7]$ and $i_N \epsilon [2,4]$.

	$n=[5,7];m=[2,4]$		
	Aslam (2019c) chart	Aslam et al. (2019a) chart	The proposed chart
c		NARL	
0	[376.88,378.16]	[376.56,372.79]	[372.31,371.37]
0.02	[373.16,372.95]	[372.74,367.42]	[368.47,365.98]
0.03	[368.6,366.63]	[368.06,360.91]	[363.77,359.44]
0.05	[354.65,347.62]	[353.73,341.33]	[349.4,339.8]
0.06	[345.6,335.54]	[344.44,328.9]	[340.07,327.34]
0.08	[324.31,307.93]	[322.6,300.53]	[318.17,298.88]
0.1	[300.14,277.85]	[297.84,269.71]	[293.34,267.97]
0.12	[274.61,247.48]	[271.72,238.68]	[267.17,236.84]
0.15	[236.41,204.54]	[232.72,195.01]	[228.11,193.03]
0.2	[179.14,145.38]	[174.48,135.38]	[169.83,133.12]
0.25	[133.58,102.49]	[128.44,92.8]	[123.77,90.24]
0.3	[99.29,72.58]	[94.08,63.7]	[89.41,60.88]
0.4	[55.63,37.61]	[51.01,30.91]	[46.42,27.9]
0.5	[32.2,20.54]	[28.55,15.93]	[24.26,13.17]
0.6	[19.35,11.85]	[16.65,8.86]	[12.87,6.57]
0.7	[12.08,7.23]	[10.18,5.36]	[7.04,3.59]
0.8	[7.85,4.67]	[6.56,3.55]	[4.06,2.22]
0.9	[5.31,3.2]	[4.46,2.56]	[2.54,1.58]
0.95	[4.44,2.71]	[3.76,2.23]	[2.1,1.4]
1	[3.75,2.34]	[3.21,1.98]	[1.78,1.27]

$ARL_{0N} \geq r_{0N}$. Several combinations exist where $ARL_{0N} \geq r_{0N}$, choose that combination of $k_{1N} \epsilon [k_{1L}, k_{1U}]$ and $k_{2N} \epsilon [k_{2L}, k_{2U}]$ where ARL_{0N} is very close to r_{0N}.

Step-2: Determine the values of $ARL_{1N} \epsilon [ARL_{1L}, ARL_{1U}]$ using the selected value of $k_{1N} \epsilon [k_{1L}, k_{1U}]$ and $k_{2N} \epsilon [k_{2L}, k_{2U}]$.

3. Advantages of the proposed chart

In this section, the advantages of the proposed $\overline{X}_N$ chart will be discussed with the existing chart using MDS proposed by Aslam et al. (2019a) and chart using repetitive sampling proposed by Aslam (2019c) under neutrosophic statistics. The efficiency of the proposed chart over the existing charts will be compared in terms of NARL.

3.1. By theoretically

To show the efficiency of the proposed chart over the control chart proposed by Aslam et al. (2019a) and Aslam (2019c), the values of NARL when $i_N = 5 + 7I_{iN}; I_{iN} \epsilon [0, 0.2857]$ and $n_N = 2 + 4I_{nN}; I_{nN} \epsilon [0, 0.5]$ are shown in Table 4 for various values of c. From Table 4, it can be noted that the proposed chart for $\overline{X}_N$ provides the smaller values of NARL as compared to the existing chart using MDS and chart using repetitive sampling. For example, when c = 0.1, the values of NARL from the proposed chart is $ARL_{1N}\epsilon\left[293.34,267.97\right]$, the values of NARL from Aslam et al. (2019a) chart is $ARL_{1N}\epsilon\left[297.84,269.71\right]$ and the values of NARL from Aslam (2019c) chart is $ARL_{1N}\epsilon\left[300.14,277.85\right]$. From the information about NARL, it can be seen that the proposed chart will detect the shift from 267th sample to 293rd sample, the chart proposed by Aslam et al. (2019a) will detect the shift in the process from 269th sample to 297th sample and the chart proposed by Aslam (2019c) will detect the shift in the process from 277th sample and 300th sample. From the study, it can be clearly noted that the proposed chart has the ability to detect the shift in the process earlier than the two existing control charts under uncertainty. From the theoretical comparisons, it can be concluded that the proposed $\overline{X}_N$ is efficient in terms of NARL as compared to the existing charts. The use of the proposed $\overline{X}_N$ in the industry will minimize the non-conforming items and will help the industry to improve the quality of the product.

3.2. By simulation

Now, the efficiency of the proposed $\overline{X}_N$ over the charts proposed by Aslam et al. (2019a) and Aslam (2019c) is shown using the data generated by the simulation. The simulated data are generated from the neutrosophic standard normal distribution. The first 20 neutrosophic observations are generated by assuming the process is in-control state and the next 30 observations are generated when the process is shifted at $c=$ 0.40. For $i_N=5+7I_{iN};I_{iN}\epsilon\left[0,0.2857\right]$, $n_N=2+4I_{nN};I_{nN}\epsilon\left[0,0.5\right]$ and $ARL_{0N}=370$, from Table 2, the values of NARL is $ARL_{1N}\epsilon\left[46.42,27.9\right]$. At this setting, it is expected that the control chart should detect the shift in the process from the 27th sample to the 46th sample. The values of the statistic $\overline{X}_N$ are computed and plotted on three control charts. Figure 1 presents the proposed chart, Figure 2 shows Aslam et al. (2019a) chart and Figure 3 shows Aslam (2019c) control chart. According to Table 2, the proposed chart should detect a shift in the process between the 27th sample and the 46th sample. From Figure 1, it can be seen that the first point beyond the outer limit is at the 27th sample. On the other hand, in Figures 2 and 3, all the plotted points are within the outer control limits that indicating that the process is in an in-control state while Figure 1 clearly indicates the shift in the process. In nutshell, by comparing Figures 1–3, it can be noted that the proposed chart in Figure 1 detects the shift before the 27th sample. On the other hand, the charts proposed by Aslam et al. (2019a) and Aslam (2019c) do not detect the shift in the process. From the study, it is concluded that the proposed chart detects the shift in the process as expected while the existing charts show that the process is an in-control state. From the study, it is concluded that the proposed chart is efficient in detecting the shift as compared to the existing charts.

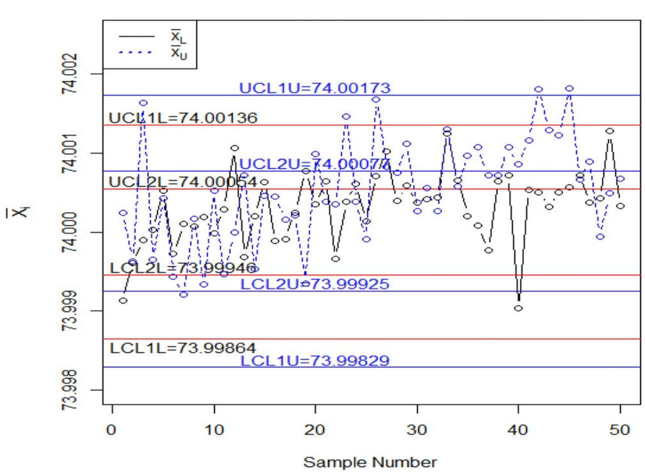

Figure 1. The propose chart using simulated data.

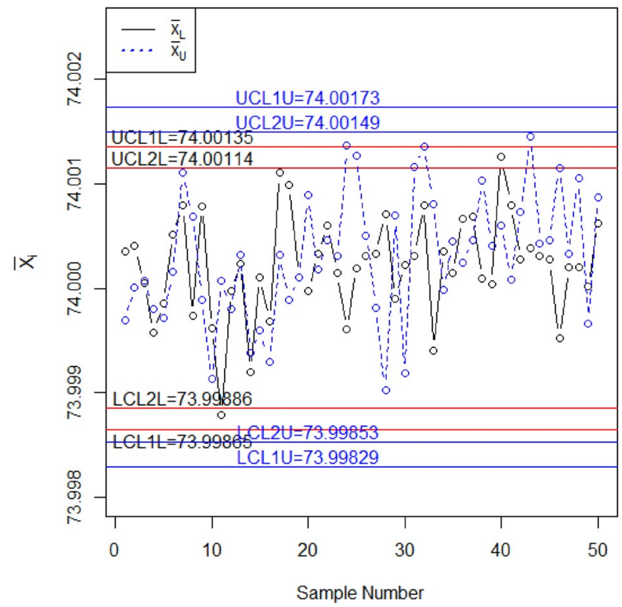

Figure 2. Aslam et al. (2019a) chart using the simulated data.

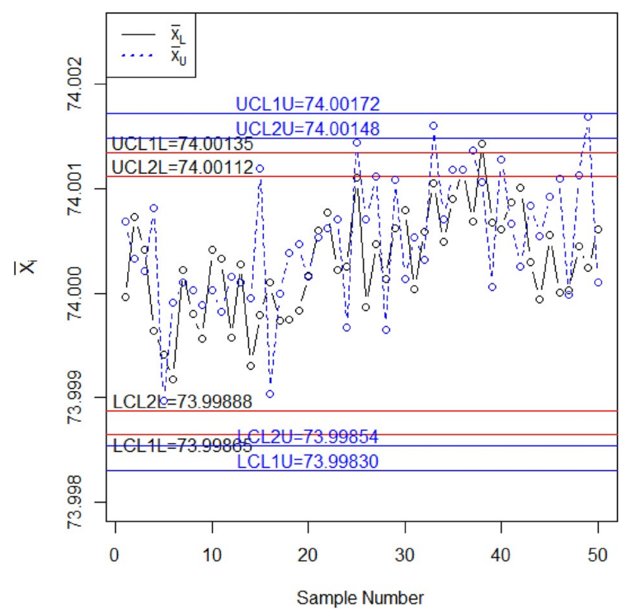

Figure 3. Aslam (2019c) chart using simulated data.

4. Monitoring road accidents and road injuries

The applications of the proposed chart and the charts proposed by Aslam et al. (2019a) and Aslam (2019c) are given with the help of road accidents and road injuries data. The road accidents and road injuries data were selected from https://data.gov.sa/Data/en/dataset/1439/resource/e6a973aa-32a8-4fa2-964c-78bcf0e8bf58.

Example 4.1

The first example is about the road accident data for the year 2019. The road accident data reported for each day of the week is taken to apply the proposed control chart and two existing control charts. The road accidents are shown in Table 5.

For $i_N \epsilon [5,7]$, $n_N \epsilon [2,4]$ and ARL_{0N} =370, the control limits for the proposed chart are calculated as follows

$$LCL_{1N} \epsilon [394.30, 389.84]$$

$$LCL_{2N} \epsilon [459.38, 443.06]$$

$$UCL_{2N} \epsilon [545.85, 527.39]$$

$$UCL_{1N} \epsilon [610.93, 580.62]$$

where $\mu_N \epsilon [502.62, 485.23]$, $\sigma_N \epsilon [79.92, 83.24]$, $k_1 \epsilon [3.0301, 3.0318]$ and $k_1 \epsilon [1.2094, 1.3400]$. The proposed control chart and charts proposed by Aslam et al. (2019a) and Aslam (2019c) are shown in Figure 4.

The left figure in Figure 4 presents the proposed chart, the middle figure in Figure 4 shows the chart proposed by Aslam et al. (2019a) and the right figure in Figure 4 presents the control chart proposed by Aslam (2019c). By comparing the three charts in Figure 1, it can be seen that the proposed chart indicates that several road accident observations are within the indeterminacy area that needs attention. On the other hand, the two existing control charts show only one observation is in the indeterminate interval. From Figure 4, it is concluded that the proposed chart can be used effectively for monitoring road accidents than the existing charts under uncertainty.

Example 4.2

The second example is about the road accident data for the year 2019. The road accident data reported by age are taken

Table 5. Road accidents in Jeddah when $n_N \epsilon [5,7]$ and $i_N \epsilon [2,4]$.

Months	Saturday	Sunday	Monday	Tuesday	Wednesday	Thursday	Friday	$\overline{X}_N$
January	426	601	596	586	574	583	407	[556.6,539]
February	487	812	525	476	421	498	413	[544.2,518.86]
March	406	789	551	427	412	498	398	[517,497.29]
April	448	614	458	407	491	486	407	[483.6,473]
May	423	611	518	457	427	482	412	[487.2,475.71]
June	530	590	563	475	479	511	372	[527.4,502.86]
July	493	623	511	587	587	528	396	[560.2,532.14]
August	453	652	579	578	552	503	427	[562.8,534.86]
September	491	546	503	498	488	517	410	[505.2,493.29]
October	378	412	422	413	382	456	373	[401.4,405.14]
November	394	533	449	380	393	405	394	[429.8,421.14]
December	402	576	517	397	388	419	307	[456,429.43]

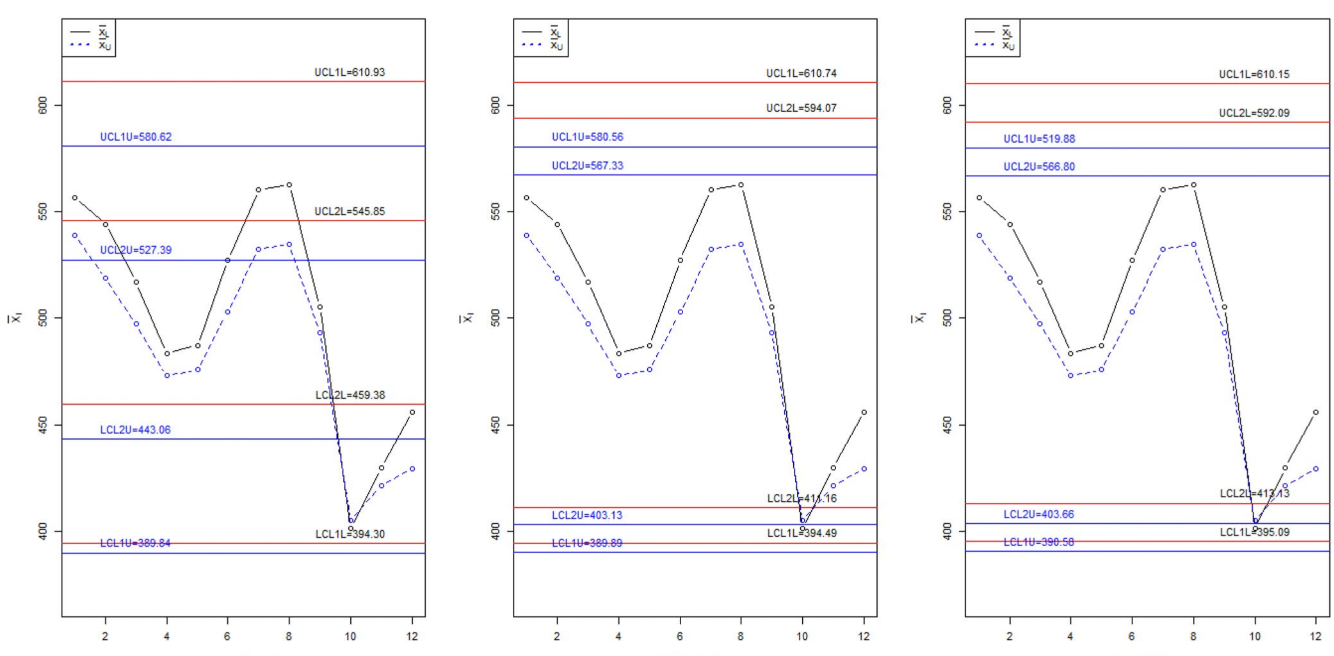

Figure 4. Control charts for road accidents data.

Table 6. Injury by age data when $n_N \epsilon [5,7]$ and $i_N \epsilon [2,4]$.

	Age					
Months	Less than 18	18 to 30	30 to 40	40 to 50	More than 50	$\overline{X}_N$
January	14	59	62	49	27	[45,42.2]
February	11	61	54	39	41	[42,41.2]
March	21	92	71	41	48	[61.33,54.6]
April	16	79	61	36	36	[52,45.6]
May	12	74	61	29	23	[49,39.8]
June	18	86	75	33	29	[59.67,48.2]
July	15	76	61	29	38	[50.67,43.8]
August	22	89	88	55	44	[66.33,59.6]
September	25	103	92	62	55	[73.33,67.4]
October	15	89	74	48	34	[59.33,52]
November	17	74	55	54	39	[48.67,47.8]
December	15	96	61	44	38	[57.33,50.8]

to apply the proposed control chart and two existing control charts. The road accidents are shown in Table 6.

For $i_N \epsilon [5,7]$, $n_N \epsilon [2,4]$ and ARL_{0N} =370, the control limits for the proposed chart are calculated as follows

$$LCL_{1N} = [-28.72, -9.99]$$

$$LCL_{2N} = [12.36, 11.70]$$

$$UCL_{2N} = [64.14, 44.19]$$

$$UCL_{2N} = [105.21, 65.88]$$

where $\mu_N \epsilon [55.39, 49.42]$, $\sigma_N \epsilon [38.39, 27.94]$, $k_1 \epsilon [3.0326, 3.0356]$ and $k_1 \epsilon [1.1725, 1.3001]$. The proposed control chart and charts proposed by Aslam et al. (2019a) and Aslam (2019c) are shown in Figure 4.

The left figure in Figure 5 presents the proposed chart, the middle figure in Figure 5 shows the chart proposed by Aslam et al. (2019a) and the right figure in Figure 5 presents the control chart proposed by Aslam (2019c). By comparing the three charts in Figure 5, it can be seen that the proposed chart indicates that all most of the road accident observations are within the indeterminacy area that needs attention. On the other hand, the two existing control charts show some observations are in indeterminate intervals. From Figure 5, it is concluded that under indeterminacy, the proposed chart effectively indicates indeterminate observations as compared to the existing charts.

5. Concluding remarks

The paper was presented for the Shewhart X-bar chart using the MDSRS under neutrosophic statistics. The proposed chart was the generalization of several control charts. The necessary measures to evaluate the performance of the proposed chart were derived under neutrosophic statistics. The efficiency of the proposed chart was compared with the

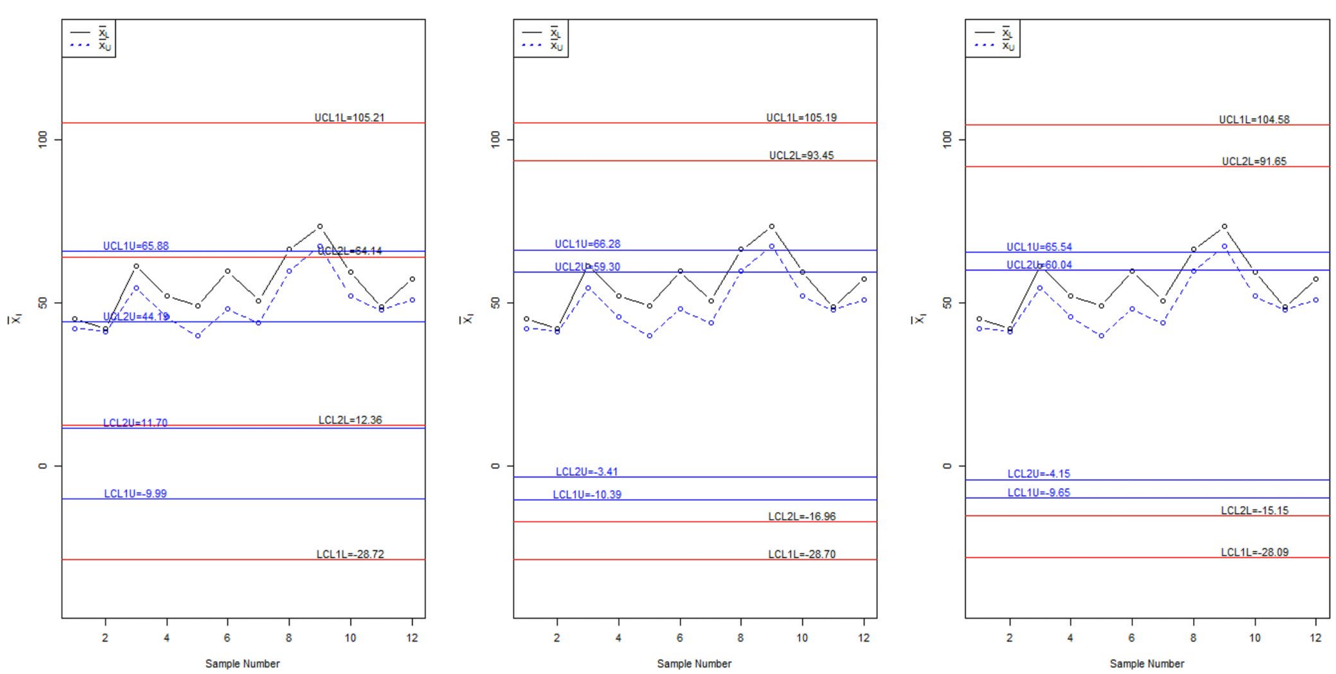

Figure 5. Control charts for injury by age data.

existing control charts using the simulated and real data sets. From the comparative studies, it can be concluded that the proposed chart performs better than the existing chart in detecting the shift in the process in an uncertain environment. The application of the proposed chart will lead to minimizing road accidents and injuries. The evaluation of the proposed chart using a cost model can be studied as future research.

Acknowledgments

The authors are deeply thankful to the editor and reviewers for their valuable suggestions to improve the quality and presentation of the paper.

Data availability

The data are given in the paper.

Disclosure statement

No potential conflict of interest was reported by the authors.

Funding

The author(s) reported there is no funding associated with the work featured in this article.

ORCID

Muhammad Aslam http://orcid.org/0000-0003-0644-1950

References

Abdel-Basset, M., Atef, A., & Smarandache, F. (2019). A hybrid neutrosophic multiple criteria group decision making approach for project selection. *Cognitive Systems Research*, *57*, 216–227. https://doi.org/10.1016/j.cogsys.2018.10.023

Abdel-Basset, M., Gunasekaran, M., Mohamed, M., & Smarandache, F. (2019). A novel method for solving the fully neutrosophic linear programming problems. *Neural Computing and Applications*, *31*(5), 1595–1605. https://doi.org/10.1007/s00521-018-3404-6

Abdel-Basset, M., Mohamed, M., & Smarandache, F. (2018). An extension of neutrosophic AHP–SWOT analysis for strategic planning and decision-making. *Symmetry*, *10*(4), 116. https://doi.org/10.3390/sym10040116

Abdel-Basset, M., Nabeeh, N. A., El-Ghareeb, H. A., & Aboelfetouh, A. (2020). Utilising neutrosophic theory to solve transition difficulties of IoT-based enterprises. *Enterprise Information Systems*, *14*(9-10), 1304–1321. https://doi.org/10.1080/17517575.2019.1633690

Adeoti, O. A. (2018). A new double exponentially weighted moving average control chart using repetitive sampling. *International Journal of Quality & Reliability Management*, *35*(2), 387–404. https://doi.org/10.1108/IJQRM-11-2016-0198

Ahmad, L., Aslam, M., & Jun, C.-H. (2014). Designing of X-bar control charts based on process capability index using repetitive sampling. *Transactions of the Institute of Measurement and Control*, *36*(3), 367–374. https://doi.org/10.1177/0142331213502070

Alakoc, N. P., & Apaydin, A. (2018). A fuzzy control chart approach for attributes and variables. *Engineering, Technology & Applied Science Research*, *8*(5), 3360–3365. https://doi.org/10.48084/etasr.2192

Aldosari, M. S., Aslam, M., & Jun, C.-H. (2017). A new attribute control chart using multiple dependent state repetitive sampling. *IEEE Access*, *5*, 6192–6197. https://doi.org/10.1109/ACCESS.2017.2687523

Aldosari, M. S., Aslam, M., Khan, N., & Jun, C.-H. (2018). Design of a new variable Shewhart control chart using multiple dependent state repetitive sampling. *Symmetry*, *10*(11), 641. https://doi.org/10.3390/sym10110641

Aldosari, M. S., Aslam, M., Khan, N., Ahmad, L., & Jun, C.-H. (2018). A new S 2 control chart using multiple dependent state repetitive sampling. *IEEE Access*, *6*, 49224–49236. https://doi.org/10.1109/ACCESS.2018.2803040

Aslam, M. (2019a). A new failure-censored reliability test using neutrosophic statistical interval method. *International Journal of Fuzzy Systems*, *21*(4), 1214–1220. https://doi.org/10.1007/s40815-018-0588-y

Aslam, M. (2019b). Attribute control chart using the repetitive sampling under neutrosophic system. *IEEE Access*, *7*, 15367–15374. https://doi.org/10.1109/ACCESS.2019.2895162

Aslam, M. (2019c). Design of X-bar control chart for resampling under uncertainty environment. *IEEE Access*, *7*, 60661–60671. https://doi.org/10.1109/ACCESS.2019.2915007

Aslam, M., & Khan, N. (2019). A new variable control chart using neutrosophic interval method-an application to automobile industry. *Journal of Intelligent & Fuzzy Systems*, *36*(3), 2615–2623. https://doi.org/10.3233/JIFS-181767

Aslam, M., Arif, O.-H., & Jun, C.-H. (2017). A control chart for gamma distribution using multiple dependent state sampling. *Industrial Engineering and Management Systems*, *16*(1), 109–117. https://doi.org/10.7232/iems.2017.16.1.109

Aslam, M., Azam, M., Khan, N., & Jun, C.-H. (2015). A control chart for an exponential distribution using multiple dependent state sampling. *Quality & Quantity*, *49*(2), 455–462. https://doi.org/10.1007/s11135-014-0002-2

Aslam, M., Bantan, R. A., & Khan, N. (2019a). Design of X-bar control chart using multiple dependent state sampling under indeterminacy environment. *IEEE Access*, *7*, 152233–152242. https://doi.org/10.1109/ACCESS.2019.2947598

Aslam, M., Bantan, R. A., & Khan, N. (2019b). Design of a new attribute control chart under neutrosophic statistics. *International Journal of Fuzzy Systems*, *21*(2), 433–440. https://doi.org/10.1007/s40815-018-0577-1

Aslam, M., Khan, N., & Khan, M. Z. (2018). Monitoring the variability in the process using neutrosophic statistical interval method. *Symmetry*, *10*(11), 562. https://doi.org/10.3390/sym10110562

Aslam, M., Nazir, A., & Jun, C.-H. (2015). A new attribute control chart using multiple dependent state sampling. *Transactions of the Institute of Measurement and Control*, *37*(4), 569–576. https://doi.org/10.1177/0142331214549094

Avakh Darestani, S., Moradi Tadi, A., Taheri, S., & Raeiszadeh, M. (2014). Development of fuzzy U control chart for monitoring defects. *International Journal of Quality & Reliability Management*, *31*(7), 811–821. https://doi.org/10.1108/IJQRM-03-2013-0048

Bai, D., & Lee, K. (2002). Variable sampling interval X control charts with an improved switching rule. *International Journal of Production Economics*, *76*(2), 189–199. https://doi.org/10.1016/S0925-5273(01)00161-X

Engin, O., Çelik, A., & Kaya, İ. (2008). A fuzzy approach to define sample size for attributes control chart in multistage processes: An application in engine valve manufacturing process. *Applied Soft Computing*, *8*(4), 1654–1663. https://doi.org/10.1016/j.asoc.2008.01.005

Ercan Teksen, H., & Anagun, A. S. (2018). Different methods to fuzzy X¯-R control charts used in production: Interval type-2 fuzzy set example. *Journal of Enterprise Information Management*, *31*(6), 848–866. https://doi.org/10.1108/JEIM-01-2018-0011

Ertuğrul, İ., & Aytaç, E. (2009). Construction of quality control charts by using probability and fuzzy approaches and an application in a textile company. *Journal of Intelligent Manufacturing*, *20*(2), 139–149. https://doi.org/10.1007/s10845-008-0230-1

Ertuğrul, I., & Güneş, M. (2007). *The usage of fuzzy quality control charts to evaluate product quality and an application*. Springer. pp. 660–673.

Fadaei, S., & Pooya, A. (2018). Fuzzy U control chart based on fuzzy rules and evaluating its performance using fuzzy OC curve. *The TQM Journal*, *30*(3), 232–247. https://doi.org/10.1108/TQM-10-2017-0118

Faraz, A., Kazemzadeh, R. B., Moghadam, M. B., & Bazdar, A. (2010). Constructing a fuzzy Shewhart control chart for variables when uncertainty and randomness are combined. *Quality & Quantity*, *44*(5), 905–914. https://doi.org/10.1007/s11135-009-9244-9

Fernández, M. N. P. (2017). *Fuzzy theory and quality control charts*. IEEE.

Gülbay, M., Kahraman, C., & Ruan, D. (2004). α-Cut fuzzy control charts for linguistic data. *International Journal of Intelligent Systems*, *19*(12), 1173–1195. https://doi.org/10.1002/int.20044

He, D., Grigoryan, A., & Sigh, M. (2002). Design of double-and triple-sampling X-bar control charts using genetic algorithms. *International Journal of Production Research*, *40*(6), 1387–1404. https://doi.org/10.1080/00207540110118415

Ho, L. L., & Quinino, R. C. (2013). An attribute control chart for monitoring the variability of a process. *International Journal of Production Economics*, *145*(1), 263–267. https://doi.org/10.1016/j.ijpe.2013.04.046

Joekes, S., & Barbosa, E. P. (2013). An improved attribute control chart for monitoring non-conforming proportion in high quality processes. *Control Engineering Practice*, *21*(4), 407–412. https://doi.org/10.1016/j.conengprac.2012.12.005

Kaya, I. (2009). A genetic algorithm approach to determine the sample size for attribute control charts. *Information Sciences*, *179*(10), 1552–1566. https://doi.org/10.1016/j.ins.2008.09.024

Mojtaba Zabihinpour, S., Ariffin, M., Tang, S. H., & Azfanizam, A. (2015). Construction of fuzzy¯ XS control charts with an unbiased estimation of standard deviation for a triangular fuzzy random variable. *Journal of Intelligent & Fuzzy Systems*, *28*(6), 2735–2747. https://doi.org/10.3233/IFS-151551

Senturk, S., & Erginel, N. (2009). Development of fuzzy $\overline{X}$~-R~and $\overline{X}$~-S~control charts using α-cuts. *Information Sciences*, *179*(10), 1542–1551. https://doi.org/10.1016/j.ins.2008.09.022

Sherman, R. E. (1965). Design and evaluation of a repetitive group sampling plan. *Technometrics*, *7*(1), 11–21. https://doi.org/10.1080/00401706.1965.10490222

Smarandache, F. (2010). Neutrosophic Logic-A Generalization of the Intuitionistic Fuzzy Logic. Multispace & Multistructure Neutrosophic Transdisciplinarity. *Collected Papers of Science)*, *4*(100), 396.

Smarandache, F. (2014). *Introduction to neutrosophic statistics*. Infinite Study.

Wu, Z., & Wang, Q. (2007). An np control chart using double inspections. *Journal of Applied Statistics*, *34*(7), 843–855. https://doi.org/10.1080/02664760701523492

Zarandi, M. F., Alaeddini, A., & Turksen, I. (2008). A hybrid fuzzy adaptive sampling–run rules for Shewhart control charts. *Information Sciences*, *178*(4), 1152–1170. https://doi.org/10.1016/j.ins.2007.09.028